Appl. Math. Mech. -Engl. Ed., **36**(11), 1449–1458 (2015)
DOI 10.1007/s10483-015-1995-7

Applied Mathematics and Mechanics (English Edition)

Investigation of third-grade non-Newtonian blood flow in arteries under periodic body acceleration using multi-step differential transformation method*

M. HATAMI[1], S. E. GHASEMI[2], S. A. R. SAHEBI[3], S. MOSAYEBIDORCHEH[4], D. D. GANJI[4], J. HATAMI[5,†]

1. Department of Mechanical Engineering, Esfarayen University of Technology, North Khorasan 49137, Iran;
2. Young Researchers and Elite Club, Islamic Azad University, Qaemshahr 47649, Iran;
3. Deptartment of Mechanical Engineering, Islamic Azad University, Sari Mazandaran 47416, Iran;
4. Department of Mechanical Engineering, Babol University of Technology, Babol 47148, Iran;
5. Garmsar Health & Care Center, Semnan University of Medical Sciences, Semnan 35131, Iran

Abstract In this paper, a non-Newtonian third-grade blood in coronary and femoral arteries is simulated analytically and numerically. The blood is considered as the third-grade non-Newtonian fluid under the periodic body acceleration motion and the pulsatile pressure gradient. The hybrid multi-step differential transformation method (Hybrid-Ms-DTM) and the Crank-Nicholson method (CNM) are used to solve the partial differential equation (PDE), and a good agreement between them is observed in the results. The effects of the some physical parameters such as the amplitude, the lead angle, and the body acceleration frequency on the velocity and shear stress profiles are considered. The results show that increasing the amplitude, A_{g}, and reducing the lead angle of body acceleration, φ, make higher velocity profiles on the center line of both arteries. Also, the maximum wall shear stress increases when A_{g} increases.

Key words pulsatile blood, third-grade non-Newtonian fluid, differential transformation method (DTM), femoral artery, coronary artery

Chinese Library Classification O37
2010 Mathematics Subject Classification 76A05

1 Introduction

Non-Newtonian fluids have many applications, especially in biomedical science. For example, blood can be a non-Newtonian fluid whose physical properties have been presented by Abdel Baieth[1]. Blood is composed of plasma, red and white blood cells, platelets, etc., and can be considered as one of the most important multi-component mixtures occurring in nature. Ogulu and Amos[2] modeled the pulsatile blood flow in the cardiovascular system employing the Navier-Stokes equation, and found an increase in the wall shear stress when the porosity of the medium was increased. Praveen-Kumar et al.[3] investigated the effects of gold nanoparticles in blood from the biomedical viewpoint by experiments. Hatami et al.[4] studied the third-grade

* Received Sept. 25, 2014 / Revised Jun. 3, 2015
† Corresponding author, E-mail: javad.hatamy@gmail.com

non-Newtonian blood conveying gold nanoparticles in a porous and hollow vessel by two analytical methods called the least square method (LSM) and the Galerkin method (GM). They considered temperature dependency on the blood by Vogel's model and investigated the effect of Brownian motion and magnetohydrodynamics (MHD) on the nanoparticles in the blood flow. Moyers-Gonzalez et al.[5] focused on the modeling of the oscillatory blood flow in a tube, and observed that as the frequency of the pressure gradient oscillations increases, the peak values of the velocity field and shear stress decrease.

The characteristics of flow and heat transfer of the second-grade viscoelastic electrically conducting blood in a channel with oscillatory stretching walls in the presence of an externally applied magnetic field were investigated by Misra et al.[6]. Massoudi and Phuoc[7] modeled blood as a modified second-grade fluid where the viscosity and the normal stress coefficients depend on the shear rate. They considered the Fahraeus-Lindqvist effect which assumes that the blood near the wall behaves as a Newtonian fluid, whereas in the core as a non-Newtonian fluid. In a pioneering study, Majhi and Nair[8] mathematically modeled the pulsatile blood flow subjected to the externally-imposed periodic body acceleration by considering the blood as a third-grade fluid using the numerical Crank-Nicholson method (CNM).

As mentioned before, blood can be assumed as a non-Newtonian fluid, and so many studies focused on second-grade and third-grade non-Newtonian fluids. The modeling and solution of the unsteady flow of an incompressible third-grade fluid over a porous plate within a porous medium were investigated by Aziz and Aziz[9]. They considered that the fluid was electrically conducting in the presence of a uniform magnetic field applied transversely to the flow. The MHD flow due to the non-coaxial rotations of a porous disk, moving with a uniform acceleration in its own plane and a second-grade fluid at infinity, was examined by Asghar et al.[10]. Keimanesha et al.[11] solved the problem of a third-grade non-Newtonian fluid flow between two parallel plates by the multi-step differential transformation method (Ms-DTM). The influence of the third-grade, partial slip, and other thermophysical parameters on the steady flow, heat and mass transfer of the viscoelastic third-grade fluid past an infinite vertical insulated plate subject to suction across the boundary layer has been investigated by Baoku et al.[12]. Hayat et al.[13–16] discussed the treatment of third-grade non-Newtonian fluids in different applications. Ellahi et al.[17–18] discussed the third-grade non-Newtonian nanofluid in the porous media between the same two cylinders as Hatami and Ganji[19] have presented.

The concept of the differential transformation method (DTM) was first introduced by Zhou[20] in 1986. Ghasemi et al.[21–22] used the DTM for solving the nonlinear temperature distribution equation in solid and porous longitudinal fins. Ms-DTM, which is a modified form and the classical DTM, can be a suitable method for this kind of engineering and physical problems. This method was newly used in some engineering problems[23–26]. The main aim of this paper is the application of the hybrid Ms-DTM to simulate the problem of the third-grade non-Newtonian blood flow in arteries under a periodic body acceleration and compare the results with those obtained by the CNM. Therefore, the novelty of this study is the utilization of the hybrid-Ms-DTM as a powerful and the efficient technique for the blood flow analysis in femoral and coronary arteries. Also, the effects of some parameters such as the frequency, the amplitude, the lead angle of body acceleration motion, and the pulsatile pressure gradient on the velocity profiles are examined.

2 Description of problem

Consider an unsteady, incompressible, and non-Newtonian blood as a third-grade fluid in an artery. Table 1 shows the properties of the blood as a kind of non-Newtonian fluids. The flow is considered to take place axially through the circular tube of radius R under a periodic body acceleration and a pulsatile pressure gradient. The Cauchy stress in a third-grade fluid is

$$\tau = -pI + \mu A_1 + \alpha_1 A_2 + \alpha_2 A_1^2 + \beta_1 A_3 + \beta_2 (A_1 A_2 + A_2 A_1) + \beta_3 (\mathrm{tr} A_1^2) A_1, \tag{1}$$

Table 1 Some properties of non-Newtonian blood[1,8]

Specification	$\rho/(\mathrm{kg\cdot m^{-3}})$	$C_p/(\mathrm{J\cdot kg^{-1}\cdot K^{-1}})$	$k/(\mathrm{W\cdot m^{-1}\cdot K^{-1}})$	μ	β
Blood	1 060	3 617	0.52	0.003	0.001

where $-pI$ denotes the spherical stress due to the restraint of incompressibility, and α_1, α_2, β_1, β_2, and β_3 are the material modules and are considered to be functions of temperature generally. In (1), the kinematical tensors A_1, A_2, and A_3 can be defined by[8]

$$A_1 = (\nabla V) + (\nabla V)^{\mathrm{T}}, \tag{2}$$

$$A_n = \frac{\mathrm{d}A_{n-1}}{\mathrm{d}t} + A_{n-1}(\nabla V) + (\nabla V)^{\mathrm{T}} A_{n-1}, \quad n = 2, 3, \tag{3}$$

where $V = (0, 0, v(r))$ denotes the velocity field, the superscript T stands for the matrix transposition, and $\frac{\mathrm{d}}{\mathrm{d}t}$ is the material time derivative defined by

$$\frac{\mathrm{d}(\cdot)}{\mathrm{d}t} = \frac{\partial(\cdot)}{\partial t} + (\mathrm{grad}(\cdot))V. \tag{4}$$

The momentum equation for an incompressible, unsteady, axi-symmetric (with the z-axis as the symmetry axis) and fully developed flow[27] in a cylindrical polar coordinate (r, θ, z) is

$$\rho\frac{\partial \bar{u}}{\partial t} = \frac{\partial p}{\partial z} + \rho G + \frac{1}{\bar{r}}\frac{\partial}{\partial \bar{r}}(\bar{r}\tau_{rz}), \tag{5}$$

where ρ, $\bar{u}$, p, τ_{rz}, t, and G denote the density, the axial velocity, the pressure, the shear stress, the time, and the body acceleration in the axial direction, respectively. The shear stress τ_{rz} for a third-grade fluid in an axi-symmetric and thermodynamically compatible flow situation can be written as

$$\tau_{rz} = \Big(\mu + \beta\Big(\frac{\partial \bar{u}}{\partial \bar{r}}\Big)^2\Big)\frac{\partial \bar{u}}{\partial \bar{r}}. \tag{6}$$

In human beings, the pressure gradient $\frac{\partial p}{\partial z}$ produced by the pumping action of the heart takes the approximate form[28]

$$-\frac{\partial p}{\partial z} = A_0 + A_1\cos(\omega_{\mathrm{p}} t), \tag{7}$$

where the circular frequency $\omega_{\mathrm{p}} = 2\pi f_{\mathrm{p}}$, and A_0, A_1, and f_{p} are the constant component of the pressure gradient, the amplitude of the fluctuating component (giving rise to the systolic and diastolic pressures), and the pulse frequency, respectively. The body acceleration G is assumed to be

$$G = A_{\mathrm{g}}\cos(\omega_{\mathrm{b}} t + \phi), \tag{8}$$

where A_{g} is the amplitude, $\omega_{\mathrm{b}} = 2\pi f_{\mathrm{b}}$, f_{b} is the frequency, and ϕ is the lead angle of G with respect to the heart action. By using (6)–(8), (5) can be written as

$$\rho\frac{\partial \bar{u}}{\partial t} = A_0 + A_1\cos(\omega_{\mathrm{p}} t) + \rho A_{\mathrm{g}}\cos(\omega_{\mathrm{b}} t + \phi) + \frac{1}{\bar{r}}\frac{\partial}{\partial \bar{r}}\Big(\bar{r}\Big(\mu + \beta\Big(\frac{\partial \bar{u}}{\partial \bar{r}}\Big)^2\Big)\frac{\partial \bar{u}}{\partial \bar{r}}\Big) \tag{9}$$

with the corresponding initial and boundary conditions

$$\bar{r} = R, \quad \bar{u} = 0; \quad \bar{r} = 0, \quad \frac{\partial \bar{u}}{\partial \bar{r}} = 0; \quad t = 0, \quad \bar{u} = 0. \tag{10}$$

The initial condition is essential for the numerical scheme adapted to estimate the time at which the pulsatile steady state sets in. The non-dimensional forms of (9)–(10) are, respectively,

$$\frac{\alpha^2}{2\pi}\frac{\partial u}{\partial T} = B_1(1+e\cos(2\pi T)) + B_2\cos(2\pi\omega_{\mathrm{r}}T+\phi) + \frac{1}{r}\frac{\partial}{\partial r}\Big(r\frac{\partial u}{\partial r}\Big(1+B\Big(\frac{\partial u}{\partial r}\Big)^2\Big)\Big), \tag{11}$$

$$r=1, \quad u=0; \quad r=0, \quad \frac{\partial u}{\partial r}=0; \quad T=0, \quad u=0, \tag{12}$$

where

$$\begin{cases} \alpha^2 = \dfrac{\rho\omega_{\mathrm{p}}R^2}{\mu}, \quad B_1 = \dfrac{A_0R^2}{\mu u_0}, \quad B_2 = \dfrac{\rho A_{\mathrm{g}}R^2}{\mu u_0}, \quad B = \dfrac{\beta u_0^2}{\mu R^2}, \\ \omega_{\mathrm{r}} = \dfrac{\omega_{\mathrm{b}}}{\omega_{\mathrm{p}}}, \quad u = \dfrac{\bar{u}}{u_0}, \quad r = \dfrac{\bar{r}}{R}, \quad T = \dfrac{\omega_{\mathrm{p}}t}{2\pi}, \quad e = \dfrac{A_1}{A_0}, \quad u_0 = \dfrac{A_0R^2}{8\mu}. \end{cases} \tag{13}$$

Here, u_0 is the cross-sectional average velocity of the flow under the steady state pressure gradient A_0. The second order non-linear partial differential (11) with the boundary conditions (12) should be solved by efficient analytical or numerical methods.

3 Applied methods

3.1 Ms-DTM

Consider a general equation of the nth-order ordinary differential equation,

$$f(t, y, y', \cdots, y^{(n)}) = 0 \tag{14}$$

subject to the initial conditions

$$y^{(k)}(0) = d_k, \quad k = 0, 1, \cdots, n-1. \tag{15}$$

To illustrate the DTM to solve the differential equations, the basic definitions of the differential transformation are introduced as follows. Let $y(t)$ be analytic in a domain D, and let $t = t_0$ represent any point in D. The function $y(t)$ is then represented by one power series whose centre is located at t_0. The differential transformation of the kth derivative of a function $y(t)$ is defined by

$$Y(k) = \frac{1}{k!}\Big(\frac{\mathrm{d}^k y(t)}{\mathrm{d}t^k}\Big)_{t=t_0}, \quad \forall t \in D. \tag{16}$$

In (16), $y(t)$ is the original function, and $Y(k)$ is the transformed function. As in Ref. [20], the differential inverse transformation of $Y(k)$ is defined by

$$y(t) = \sum_{k=0}^{\infty} Y(k)(t-t_0)^k, \quad \forall t \in D. \tag{17}$$

In fact, from (16) and (17), we obtain

$$y(t) = \sum_{k=0}^{\infty} \frac{(t-t_0)^k}{k!}\Big(\frac{\mathrm{d}^k y(t)}{\mathrm{d}t^k}\Big)_{t=t_0}, \quad \forall t \in D. \tag{18}$$

(18) implies that the concept of the differential transformation is derived from the Taylor series expansion. From the definitions of (16) and (17), it is easy to prove that the transformed functions comply with the following basic mathematics operations (see Table 2).

Table 2 Some fundamental operations of DTM and Ms-DTM

Original function	DTM	Ms-DTM
$f(t)=g(t)\pm s(t)$	$F(k)=G(k)\pm S(k)$	$F(k)=G(k)\pm S(k)$
$f(t)=cg(t)$	$F(k)=cG(k)$	$F(k)=cG(k)$
$f(t)=\dfrac{\mathrm{d}^n g(t)}{\mathrm{d}t^n}$	$F(k)=\dfrac{(k+n)!}{k!}G(k+n)$	$F(k)=\dfrac{(k+n)!}{H^n k!}G(k+n)$
$f(t)=g(t)s(t)$	$F(k)=\sum\limits_{r=0}^{k}G(r)S(k-r)$	$F(k)=\sum\limits_{r=0}^{k}G(r)S(k-r)$

In real applications, the function $y(t)$ is expressed by a finite series, and (18) can be written as

$$y(t)=\sum_{k=0}^{N}Y(k)(t-t_0)^k,\quad \forall t\in D. \tag{19}$$

(19) implies that $\sum\limits_{k=N+1}^{\infty}Y(k)(t-t_0)^k$ is negligibly small.

Let $[0,\,T]$ be the interval over which we want to find the solution of the initial value problem (11). In actual applications of the DTM, the approximate solutions of the initial and boundary value problems (11)–(12) can be expressed by the finite series

$$y(t)=\sum_{k=0}^{N}b_k t^k,\quad t\in[0,T]. \tag{20}$$

Assume that the interval $[0,T]$ is divided into N subintervals $[t_{i-1},t_i]$, $i=1,2,\cdots,M$, using the nodes $t_i=ih$, where $h=\frac{T}{M}$. The main ideas of the Ms-DTM are as follows[24]. We apply the DTM to (14) over the interval $[0,t_1]$, leading to the following approximate solution:

$$y_1(t)=\sum_{k=0}^{N}b_{1k}t^k,\quad t\in[0,t_1], \tag{21}$$

using the initial conditions $y_1^{(k)}(0)=d_k$. For $i\geqslant 2$, at each subinterval $[t_{i-1},t_i]$, we will use the initial conditions $y_i^{(k)}(t_{i-1})=y_{i-1}^{(k)}(t_{i-1})$ and apply the DTM to (14) over the interval $[t_{i-1},t_i]$, where t_0 in (16) is replaced by t_{i-1}. For the solution $y(t)$, the process is repeated and generates a sequence of approximate solutions $y_i(t),\ i=1,2,\cdots,M$,

$$y_i(t)=\sum_{k=0}^{N}b_{ik}(t-t_{i-1})^k,\quad t\in[t_{i-1},t_i]. \tag{22}$$

In fact, from the Ms-DTM, we get the following solution:

$$y(t)=\begin{cases}y_0(t), & t\in[0,t_1],\\ y_1(t), & t\in[t_1,t_2],\\ \quad\vdots & \\ y_M(t), & t\in[t_M,t_{M+1}].\end{cases} \tag{23}$$

3.2 CNM

It is obvious that the type of the current problem is the partial differential equation (PDE) with boundary and initial conditions, and the appropriate method needs to be selected. One of the available numerical sub-methods in the MAPLE 15.0[29] is the CNM. The CNM or the centered time centered space method is an implicit single stage method that can be used to find the solutions to PDEs that are first-order in time and arbitrary order in space with mixed partial derivatives. This method is an implicit scheme, and is unconditionally stable for many

problems which have the $O(h^2, k^2)$ accuracy, where h is used as the space step, and k is used as the time step. In the MAPLE software, the scheme used to compute the value at the mesh point $[1, i]$ is the result of applying central differencing to the PDE about the point $t + \frac{1}{2}k$, x_i using $1 + 2\text{ceil}\left(\frac{1}{2}x \text{ or } d\right)$ points (that is, the mesh uses ceil $\left(\frac{1}{2}x \text{ or } d\right)$ points on either side of the center). As mentioned before, Majhi and Nair[8] modeled the blood flow under the body acceleration by the current method.

4 Results and discussion

In this study, the analytical hybrid-DTM is used for the non-dimensional time (T) and the r direction to obtain the solution of (11) with the boundary condition (12). The hybrid-DTM, which is the combination of the finite difference method (FDM) and the Ms-DTM, can solve the PDEs easily. In order to proceed with its computations, the FDM is applied to the uniform points in the T, and the Ms-DTM is based on the r (non-dimensional radius) direction, and the solutions are performed. The obtained results by the hybrid-DTM are compared with the CNM[8] in Fig. 1 which shows an excellent agreement between the analytical and numerical methods. In this paper, two different arteries are considered, i.e., femoral and coronary arteries. Femoral and coronary arteries have the diameters 1 cm and 0.3 cm, respectively. Also, the constant components of the pressure gradient, A_0, for coronary and femoral arteries are taken as 698.65×10^{-3} N·m^{-1} and 32×10^{-3} N·m^{-1}, respectively, as presented by Mcdonald[30]. In the whole solution, the physical properties of blood are considered to be constant as listed in Table 1, and g is the acceleration due to gravity which is considered to be 10 m/s^2. The comparison between the hybrid-DTM and the CNM[8] is depicted in Fig. 1 for both femoral and coronary arteries when $\varphi = 0$, $e = \omega_r = 1$, $A_g = g$, and $f_b = 1.2$ Hz at various time. As seen in Fig. 1, the hybrid-DTM excellently agrees with the previous method. This is necessary to inform that increasing the time makes negative values for the velocity due to the fluctuation of the flow. Then, continue to increase the time, and the velocity will increase and reach positive values. This process occurs continuously.

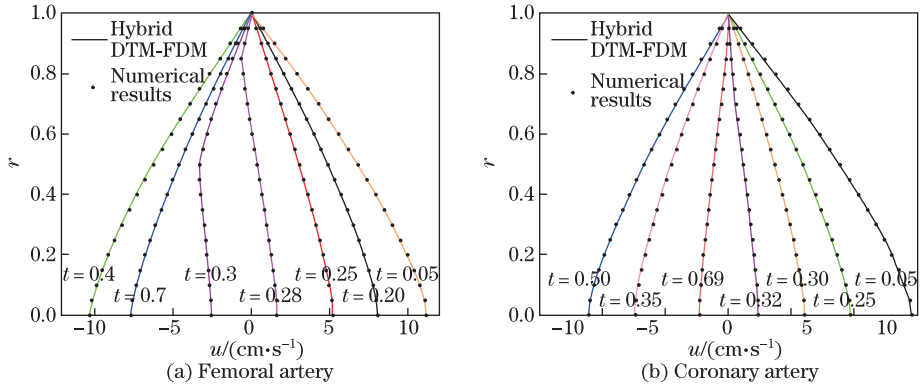

(a) Femoral artery (b) Coronary artery

Fig. 1 Comparison between hybrid-DTM (present study) with CNM[8] when $\varphi = 0$, $e = \omega_r = 1$, $A_g = g$, and $f_b = 1.2$ Hz

For better perception, Fig. 2 is depicted for coronary and femoral arteries, which shows the velocity versus time in different radii. As it can be seen, the maximum velocities occur at the center of tube ($r = 0$), and in the whole domain, it has a fluctuating nature. Also, it is obvious that when the velocity becomes negative, the maximum value is seen in the region beyond the center and near the tube wall, and the maximum values take place in lower time duration compared with positive values. Figure 3 is depicted for femoral and coronary arteries, and demonstrates the A_g effects on the velocity profiles. It can be concluded that increasing the amplitude, A_g, makes higher velocity profiles in both negative and positive values. These

effects on the velocity and wall shear stress during the time view point are presented in Fig. 4 for femoral artery when $\varphi = \pi/6$, $e = 20$, $\omega_{\mathrm{r}} = 1$, and $f_{\mathrm{b}} = 1.2$ Hz. As A_{g} increases, the maximum magnitude of the velocity along the axis increases and assumes both positive and negative values during a cycle. Also, the maximum wall shear stress increases when A_{g} increases. These effects are also observed for coronary artery (see Fig. 5). The curves are much nearer to a parabolic or convex/concave profile shape.

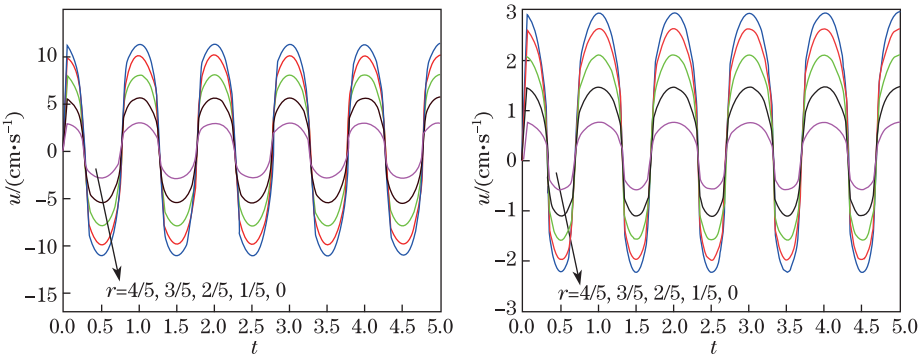

(a) Femoral artery (b) Coronary artery

Fig. 2 Velocity profiles versus time in different radii for femoral and coronary arteries when $\varphi = 0$, $e = \omega_{\mathrm{r}} = 1$, $A_{\mathrm{g}} = g$, and $f_{\mathrm{b}} = 1.2$

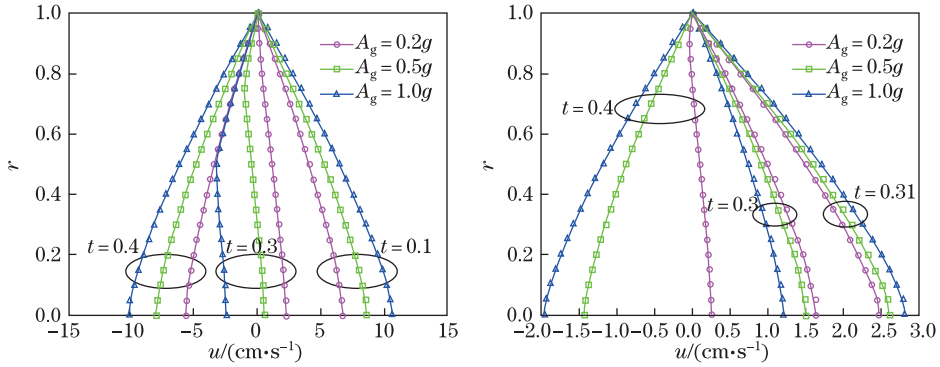

(a) Femoral artery (b) Coronary artery

Fig. 3 Velocity profiles versus radius in different times for showing effect of A_{g} when $\varphi = 0$, $e = \omega_{\mathrm{r}} = 1$, and $f_{\mathrm{b}} = 1.2$ Hz for femoral and coronary arteries

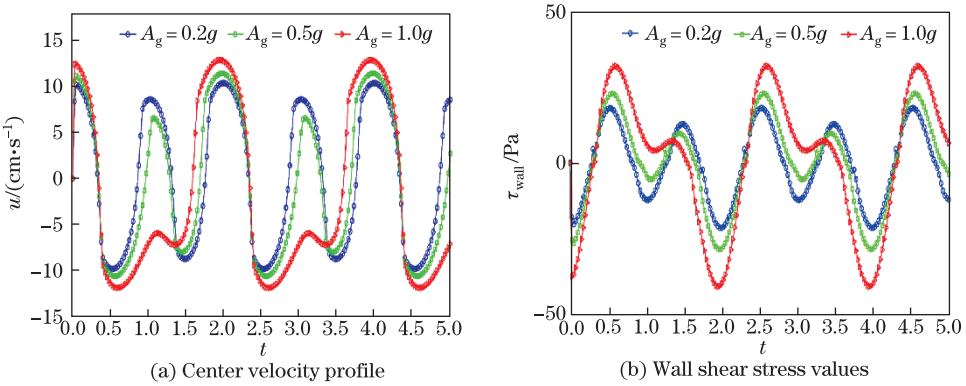

(a) Center velocity profile (b) Wall shear stress values

Fig. 4 Effect of A_{g} for femoral artery on center velocity profile and wall shear stress values when $\varphi = \pi/6$, $e = 20$, and $f_{\mathrm{b}} = 1.2$ Hz

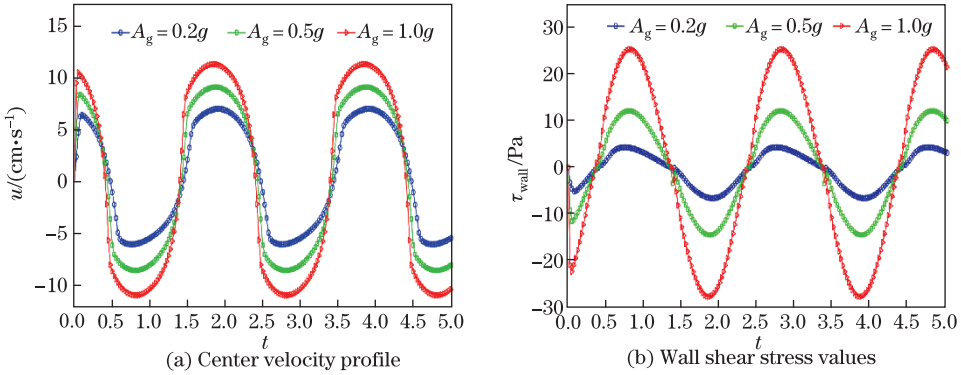

(a) Center velocity profile (b) Wall shear stress values

Fig. 5 Effect of A_g for coronary artery on center velocity profile and wall shear stress values when $\varphi = \pi/6$, $e = 1$, and $f_b = 1.2$ Hz

Finally, the effects of ω_r on the center velocity profile and the wall shear stress for femoral and coronary arteries are depicted in Figs. 6 and 7, respectively. It is seen that the changes of ω_r make a mutation in the velocity profiles, and completely change the amplitude, shape, maximum values, etc. Reducing ω_r from 1.0 to 0.5 makes a shift to the right-hand side in the maximum points in both the velocity and shear stress profiles. Also, it makes a reduction for the velocity positive maximum values and increases its negative values. Its treatment for the shear stress is completely vice versa, i.e., the increase in its positive maximum values and the decrease in its negative values. Furthermore, when $\omega_r = 0.5$, all the graphs have a relative maximum/minimum point and an absolute optimum point.

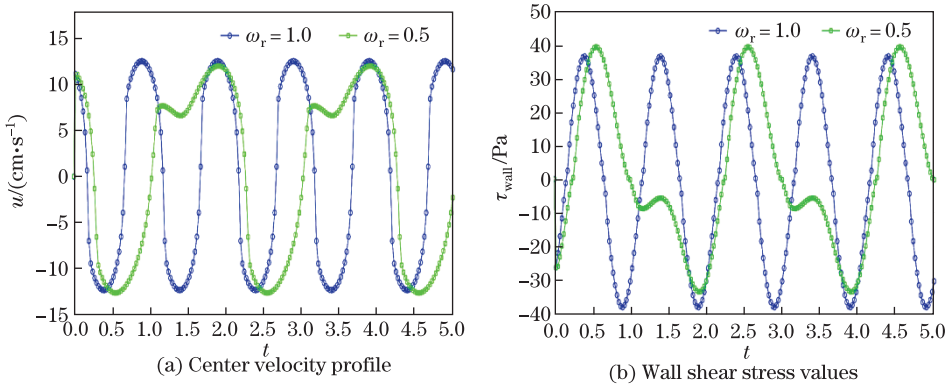

(a) Center velocity profile (b) Wall shear stress values

Fig. 6 Effect of ω_r for femoral artery on center velocity profile and wall shear stress values when $\varphi = \pi/3$, $e = 20$, and $f_b = 1.2$ Hz

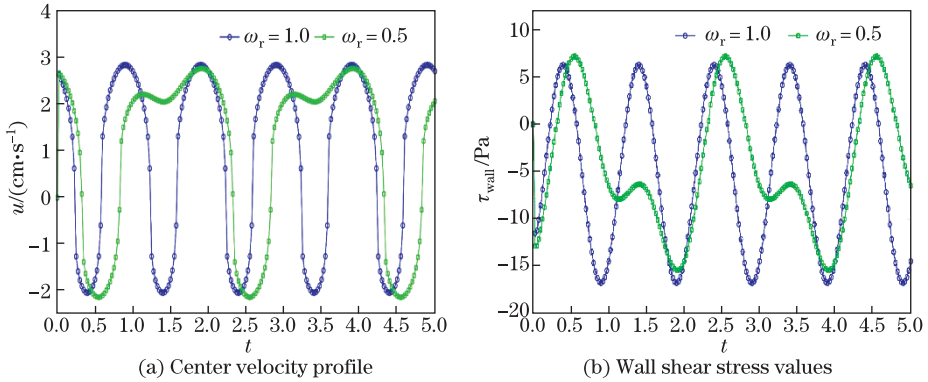

(a) Center velocity profile (b) Wall shear stress values

Fig. 7 Effect of ω_r for coronary artery on center velocity profile and wall shear stress values when $\varphi = \pi/3$, $e = 1$, and $f_b = 1.2$ Hz

5 Conclusions

In this paper, an analytical approach called the hybrid-DTM, which is the combination of the Ms-DTM and the FDM methods, has been successfully used to find the most accurate solution for the blood flow analysis in femoral and coronary arteries. The blood is considered as a third-grade non-Newtonian fluid under a periodic body acceleration and a pulsatile pressure gradient. The obtained results are compared with those of the CNM, and an excellent agreement between these two methods is observed. Thus, the hybrid-DTM due to its high accuracy and simplicity can be used in PDEs, especially in engineering and biomedicine problems. As a main outcome from the present study, it can be concluded that increasing the amplitude A_{g} and reducing the lead angle of body acceleration φ make larger velocity values. Also, the maximum wall shear stress increases when A_{g} increases.

References

[1] Abdel Baieth, H. E. Physical parameters of blood as a non-Newtonian fluid. *International Journal of Biomedical Sciences*, **4**, 323–329 (2008)

[2] Ogulu, A. and Amos, E. Modeling pulsatile blood flow within a homogeneous porous bed in the presence of a uniform magnetic field and time-dependent suction. *International Communications in Heat and Mass Transfer*, **34**, 989–995 (2007)

[3] Praveen-Kumar, K., Paul, W., and Sharma, C. P. Green synthesis of gold nanoparticles with Zingiber officinale extract: characterization and blood compatibility. *Process Biochemistry*, **46**, 2007–2013 (2011)

[4] Hatami, M., Hatami, J., and Ganji, D. D. Computer simulation of MHD blood conveying gold nanoparticles as a third-grade non-Newtonian nanofluid in a hollow porous vessel. *Computer Methods and Programs in Biomedicine*, **113**, 632–641 (2014)

[5] Moyers-Gonzalez, M. A., Owens, R. G., and Fang, J. A non-homogeneous constitutive model for human blood, part III: oscillatory flow. *Journal of Non-Newtonian Fluid Mechanics*, **155**, 161–173 (2008)

[6] Misra, J. C., Shit, G. C., Chandra, S., and Kundu, P. K. Hydromagnetic flow and heat transfer of a second-grade viscoelastic fluid in a channelwith oscillatory stretching walls: application to the dynamics of blood flow. *Journal of Engineering Mathematics*, **69**, 91–100 (2011)

[7] Massoudi, M. and Phuoc, T. X. Pulsatile flow of blood using a modified second-grade fluid model. *Computers and Mathematics with Applications*, **56**, 199–211 (2008)

[8] Majhi, S. N. and Nair, V. R. Pulsatile flow of third-grade fluids under body acceleration-modelling blood flow. *International Journal of Engineering Science*, **32**, 839–846 (1994)

[9] Aziz, A. and Aziz, T. MHD flow of a third-grade fluid in a porous half space with plate suction or injection: an analytical approach. *Applied Mathematics and Computation*, **218**, 10443–10453 (2012)

[10] Asghar, S., Hanif, K., Hayat, T., and Khalique, C. M. MHD non-Newtonian flow due to non-coaxial rotations of an accelerated disk and a fluid at infinity. *Communications in Nonlinear Science and Numerical Simulation*, **12**, 465–485 (2007)

[11] Keimanesha, M., Rashidi, M. M., Chamkha, A. J., and Jafari, R. Study of a third-grade non-Newtonian fluid flow between two parallel plates using the multi-step differential transform method. *Computers and Mathematics with Applications*, **62**, 2871–2891 (2011)

[12] Baoku, I. G., Olajuwon, B. I., and Mustapha, A. O. Heat and mass transfer on a MHD third-grade fluid with partial slip flow past an infinite vertical insulated porous plate in a porous medium. *International Journal of Heat and Fluid Flow*, **40**, 81–88 (2013)

[13] Hayat, T., Shafiq, A., Alsaedi, A., and Awais, M. MHD axisymmetric flow of third-grade fluid between stretching sheets with heat transfer. *Computers and Fluids*, **86**, 103–108 (2013)

[14] Hayat, T., Hina, S., Hendi, A. A., and Asghar, S. Effect of wall properties on the peristaltic flow of a third-grade fluid in a curved channel with heat and mass transfer. *International Journal of Heat and Mass Transfer*, **54**, 5126–5136 (2011)

[15] Hayat, T., Haroon, T., Asghar, S., and Siddiqui, A. M. MHD flow of a third-grade fluid due to eccentric rotations of a porous disk and a fluid at infinity. *International Journal of Non-Linear Mechanics*, **38**, 501–511 (2003)

[16] Hayat, T., Mustafa, M., and Asghar, S. Unsteady flow with heat and mass transfer of a third-grade fluid over a stretching surface in the presence of chemical reaction. *Nonlinear Analysis*: *Real World Applications*, **11**, 3186–3197 (2010)

[17] Ellahi, R., Raza, M., and Vafai, K. Series solutions of non-Newtonian nanofluids with Reynolds' model and Vogel's model by means of the homotopy analysis method. *Mathematical and Computer Modelling*, **55**, 1876–1891 (2012)

[18] Ellahi, R., Zeeshan, A., Vafai, K., and Rahman, H. U. Series solutions for magnetohydrodynamic flow of non-Newtonian nanofluid and heat transfer in coaxial porous cylinder with slip conditions. *Proceedings of the Institution of Mechanical Engineers*, *Part N*: *Journal of Nanoengineering and Nanosystems*, **225**, 123–132 (2011)

[19] Hatami, M. and Ganji, D. D. Heat transfer and flow analysis for SA-TiO_2 non-Newtonian nanofluid passing through the porous media between two coaxial cylinders. *Journal of Molecular Liquids*, **188**, 155–161 (2013)

[20] Zhou, J. K. *Differential Transformation Method and Its Application for Electrical Circuits*, Hauzhang University Press, Wuhan (1986)

[21] Ghasemi, S. E., Hatami, M., and Ganji, D. D. Thermal analysis of convective fin with temperature-dependent thermal conductivity and heat generation. *Case Studies in Thermal Engineering*, **4**, 1–8 (2014)

[22] Ghasemi, S. E., Valipour, P., Hatami, M., and Ganji, D. D. Heat transfer study on solid and porous convective fins with temperature-dependent heat generation using efficient analytical method. *Journal of Central South University of Technology*, **21**, 4592–4598 (2014)

[23] Rashidi, M. M., Chamkh, A. J., and Keimanesh, M. Application of multi-step differential transform method on flow of a second-grade fluid over a stretching or shrinking sheet. *American Journal of Computational Mathematics*, **6**, 119–128 (2011)

[24] Gkdon, A., Merdan, M., and Yildirim, A. Adaptive multi-step differential transformation method to solving nonlinear differential equations. *Mathematical and Computer Modelling*, **55**, 761–769 (2012)

[25] Odibat, Z. M., Bertelle, C., Aziz-Alaoui, M. A., and Duchamp, G. H. E. A multi-step differential transform method and application to non-chaotic or chaotic systems. *Computers and Mathematics with Applications*, **59**, 1462–1472 (2010)

[26] Hatami, M. and Ganji, D. D. Natural convection of sodium alginate (SA) non-Newtonian nanofluid flow between two vertical flat plates by analytical and numerical methods. *Case Studies in Thermal Engineering*, **2**, 14–22 (2014)

[27] Bird, R. B., Stewart, W. E., and Ligtfoot, E. N. *Transport Phenomena*, Wiley, New York (1960)

[28] Burton, A. C. *Physiology and Biophysics of the Circulation*, Year Book Medical Publisher, Chicago (1966)

[29] Aziz, A. *Heat Conduction with Maple*, R. T. Edwards, Philadelphia (2006)

[30] Mcdonald, D. A. *Blood Flow in Arteries*, Edward Arnold, London (1974)